

## Studies of fuelling rates of CO, CH<sub>4</sub> and oxygen in the TEXTOR tokamak

G.M. McCracken<sup>a</sup>, U. Samm<sup>b</sup>, B. Bertschinger<sup>b</sup>, V. Philipps<sup>b</sup>, R.A. Pitts<sup>a,1</sup>,  
D.H.J. Goodall<sup>a</sup>, S.J. Davies<sup>a</sup>, G. van Oost<sup>c</sup>, A. Pospieszczyk<sup>b</sup>, R. Schorn<sup>b</sup>,  
B. Schweer<sup>b</sup>, P.C. Stangeby<sup>d</sup>, G. Telesca<sup>b</sup> and G. Waidmann<sup>b</sup>

<sup>a</sup> AEA Fusion (Euratom / UKAEA Fusion Association), Abingdon, Oxon, OX14 3DB, United Kingdom

<sup>b</sup> Institut für Plasmaphysik, Association KFA Euratom KFA, D-5170 Jülich, Germany

<sup>c</sup> Ecole Royale Militaire (Association Euratom – Etat Belge), B1040 Brussels, Belgium

<sup>d</sup> University of Toronto, Institute for Aerospace Studies, Ontario, Canada, M3H 5T6

Impurity gases have been introduced into TEXTOR at well defined rates to study the fuelling process and the effect they have on the overall energy balance. It is found that carbon and oxygen, introduced as CO and CH<sub>4</sub> gases have radically different behaviour. Oxygen has a high recycling coefficient  $\approx 0.99$  whereas carbon has a low recycling coefficient  $\approx 0.3$ . The radial position of the gas source was varied from the wall to the limiter radius but this made little difference to the effect on the global plasma parameters. For very high impurity influxes of both impurities drastic changes in the edge plasma were observed and disruptions could be induced.

### 1. Introduction

Impurity transport in the plasma boundary is an important factor determining whether a given impurity influx has a significant effect on the global plasma parameters, such as central radiation and fuel dilution. Earlier experimental studies have noted that there is a wide variation in behaviour of the effective fuelling rates of different gases [1]. Whereas the light gases, helium and hydrogen, tend to have a high effective fuelling rate, heavy gases can have much lower rates. CO, CH<sub>4</sub> and the higher hydrocarbons are notable for their low effective fuelling rates. Since these species are important in their own right, being the products of chemical sputtering not only at graphite surfaces per se [2], but also on carbon contaminated metal surfaces [3], we have undertaken a detailed study of the fuelling efficiency of some of these species.

The carbon containing gases can also be used as a method of introducing carbon impurities into the plasma boundary in a precisely controlled way. Although the energy distribution is much lower than that of sputtered carbon atoms, it is comparable to that of evaporated atoms. It may therefore cast light on the processes occurring during the carbon bloom [4] or other conditions where carbon is introduced by high power deposition on limiters or target plates. We have introduced CO, CH<sub>4</sub> and O<sub>2</sub> into TEXTOR both

through a port at the wall and through a test limiter whose radius can be varied. In this paper we discuss mainly the global effects of these gases on the discharge including the effect on radiated power and  $Z_{\text{eff}}$ , and the effect that the impurity introduction has on the plasma density and temperature profiles. Local measurements of impurity fluxes at the limiter have also been made. These studies complement earlier measurements on the local transport of carbon and oxygen close to the impurity source [5,6]. Measurements are reported as a function of the gas flow rate up to the condition where a disruption is induced.

### 2. Experiment

TEXTOR has been operated using nominally steady state plasma conditions which in typical experiments were  $\bar{n}_e = 1.5\text{--}3.5 \times 10^{19} \text{ m}^{-3}$ ,  $I_p = 350 \text{ kA}$ ,  $T_e(0) = 1 \text{ keV}$ , with deuterium as the working gas. The impurity gas was injected both from the wall, using an accurately calibrated gas flow, and through a test limiter whose minor radius can be varied from the wall position ( $r = 0.52 \text{ m}$ ) to inside the main limiter radius at  $r = 0.46 \text{ m}$ , defined by the ALT II pumped limiter. ALT II is operated with the pumps open, providing a net pumping for both plasma species and impurities. A schematic of the main diagnostics of interest and of the gas puffing positions is shown in figs. 1a and 1b.

The main gas feed is controlled by a feedback loop

<sup>1</sup> Present address: CRPP-EPFL, 1015 Lausanne, Switzerland.

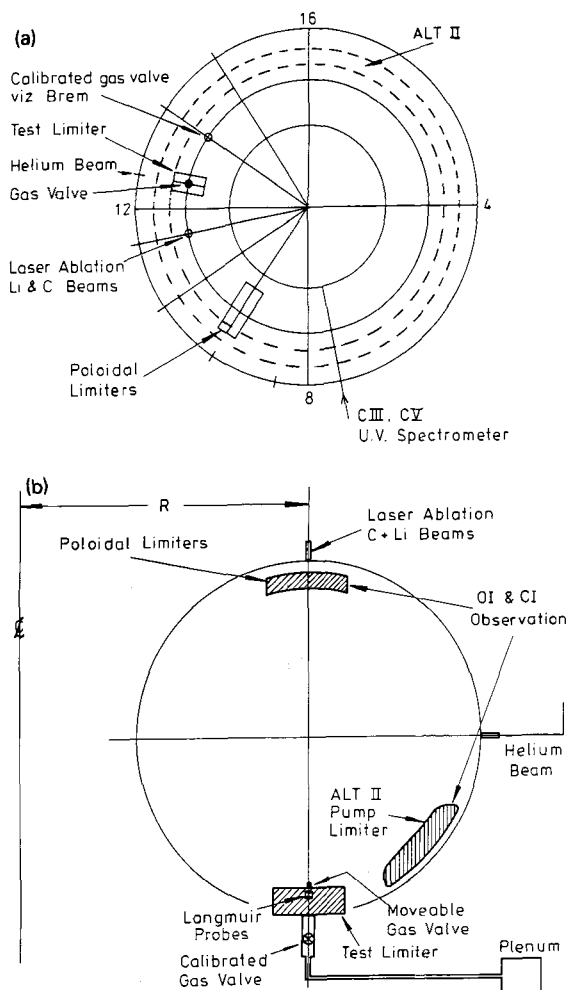


Fig. 1. (a) Top view of TEXTOR showing schematically the main components and diagnostics used in the present experiments. (b) Poloidal cross section. Diagnostics from different toroidal positions are superimposed.

to keep the line average density constant. The flow from the impurity gas valve at the wall position is calibrated to an absolute accuracy of better than 5% and the time dependence can be preprogrammed. Typically the impurity is injected at a constant rate for a period of 0.5 to 1.0 s during the steady stage period of the discharge.

The impurity fluxes are monitored at the edge using optical interference filters for OI, CI, viewing both the upper poloidal limiter and the ALT II (fig. 1b). Visible and UV spectrometers are used to measure the line integrals of suitable spectroscopic lines including CIII, CV and CVI through the plasma. The radial profile of the total radiation is measured with an eight channel bolometer array. The central  $n_e(r)$  and  $T_e(r)$  profiles are measured with an interferometer and an ECE

system, respectively. Detailed  $n_e(r)$  and  $T_e(r)$  profiles near the boundary are measured using lithium, carbon and helium beams [7,8]. In addition, local measurements of  $n_e$  and  $T_e$  were made using new Langmuir probes installed in the test limiter through which the impurity gases were introduced. A line average  $Z_{\text{eff}}$  was measured using visible bremsstrahlung [9] and a value for central  $Z_{\text{eff}}$  calculated from the plasma conductivity using the measured  $T_e(0)$ .

### 3. Results

#### 3.1. Time dependence of CO and CH<sub>4</sub>

The effect of injection of carbon monoxide in a square wave pulse from 0.8 to 1.3 s with the source at the wall is illustrated in fig. 2. The plasma current and line average density  $\bar{n}_e$  are maintained constant by feedback control from 0.5 to 2.0 s. When the gas is injected the power radiated  $P_R$ , the OI signal and the  $Z_{\text{eff}}$  increase approximately linearly. A striking difference between the behaviour of OI and CI is observed, fig. 2b. Whereas the oxygen influx increases linearly with time, indicating high recycling and effective integration of the impurities influx over the first 0.5 s, the carbon influx appears not to increase above the intrinsic background level, in fact appears to decrease slightly. Similar results are obtained for OI and CI signals at two separate viewing locations, the toroidal belt limiter and an upper poloidal limiter (fig. 1b). Over a longer time scale, puffing CO from 0.8 to 2.0 s, it is found that the OI,  $P_R$  and  $Z_{\text{eff}}$  approach a plateau, i.e. an equilibrium is established where the losses balance the constant influx. The results for the spectrometer measuring a line integral of CIII ( $\lambda = 2296 \text{ \AA}$ ) and CV ( $\lambda = 2271 \text{ \AA}$ ) through the plasma are shown in fig. 2d. The CIII increases but the CV is hardly changed. The CIII signal may be seeing transport from the primary source, see fig. 1a. The edge temperature is significantly reduced, fig. 2e, probably explaining the reduction in the overall CI. A spectrometer directly viewing the gas source shows a CIII line ( $\lambda = 464.9 \text{ nm}$ ) as a square wave pulse following the gas valve signal.

The results for methane injection are shown in fig. 3. The total gas influx is chosen as twice the rate of the CO injection in molecules per second corresponding to the same number of impurity atoms per second. The density is similar but slightly higher than in the CO discharge, fig. 3a. In this case there is no observable increase in  $Z_{\text{eff}}$ , fig. 3c, the increase in  $P_R$  is much less and both CI and OI decrease, fig. 3b. The reduction in edge temperature is also less marked, fig. 3e. However if the CH<sub>4</sub> gas puffing rate is increased further it can produce a significant increase in the power radiated and a reduction in the edge temperature. In both cases

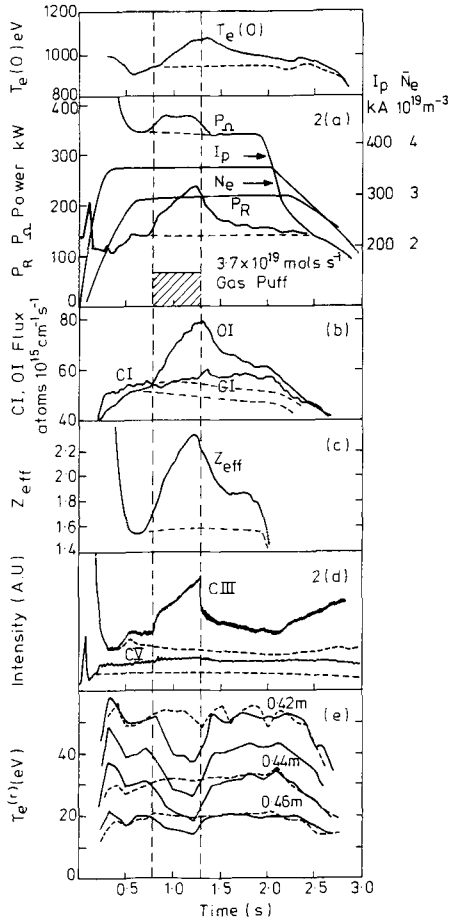


Fig. 2. CO gas injection into an ohmically heated TEXTOR plasma using the calibrated gas valve at a flow rate of  $3.7 \times 10^{19}$  molecules  $s^{-1}$ .

with sufficiently high puffing rate a plasma disruption can be induced.

The  $\Delta Z_{\text{eff}}$  can be used to estimate the number of impurity ions in the plasma if it is assumed that  $Z_{\text{eff}}$  is constant with radius. From the results in fig. 3c it is found that  $\leq 1\%$  of the number of carbon atoms injected are in the plasma. A completely independent estimate of the effective fuelling is to measure the change in the number of deuterium molecules injected, calculated from the feedback loop which maintains the constant density. It is found that 1 molecule of methane replaces  $1 \pm 0.1$  molecule of  $D_2$ , i.e. the methane is only  $\frac{1}{5}$  as effective as deuterium in fuelling electrons. If we assume, on the basis of the evidence from the methane experiment and from fig. 2, that no carbon goes in during the CO puff, then the fraction of the oxygen fluence which is in the plasma at the end of 0.5 s, based on the  $\Delta Z_{\text{eff}}$  is  $\sim 10\%$ .

### 3.2. Effect of impurity influx rate

Direct measurements of the density and temperature have been made in the region where the injected gas is being ionized. The results for different gas puff rates are shown in fig. 4. At low gas puff rates the temperature is unaltered. At gas puff rates above  $6 \times 10^{19}$  molecules  $s^{-1}$  ( $\equiv 50$  mbar) the temperature is strongly reduced. The local density is not significantly changed for even the highest gas puff rate. Since  $\bar{n}_e$  is feedback controlled this indicates that the puffing does not significantly modify the edge density gradient. At larger gas puff rates, the temperature profile is disturbed over a radial range from 0.41 to 0.46 m, as shown in fig. 2e. This marked depression must result in greater penetration of the impurities before they are ionised. At a critical gas flow rate  $\sim 10^{20}$  molecules  $s^{-1}$ , a disruption can be induced by either CO or CH<sub>4</sub>.

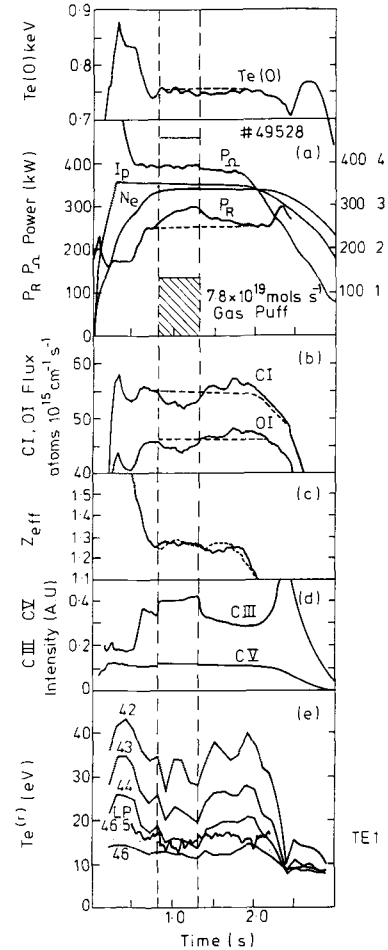


Fig. 3. CH<sub>4</sub> gas injection into an ohmically heated plasma using the calibrated valve at a flow rate of  $7.8 \times 10^{19}$  molecules  $s^{-1}$ .

#### 4. Discussion

The study of impurity gas puffing has revealed some trends which are at first quite surprising. The large difference between the behaviour of carbon and oxygen, injected in equal concentrations when injecting CO, can be understood qualitatively in terms of the difference in recycling properties. Oxygen, being a gas and forming a volatile gas with carbon, is expected to recycle at the carbon limiter with a high probability. Carbon, on the other hand, has a low reflection coefficient [10] and relatively low self-sputtering. The self-sputtering yield at normal incidence never exceeds 0.5 and for a reasonable estimate of the ion energy and charge state is likely to be  $\sim 0.35$  [2]. If we assume a simple global model for impurity recycling, similar to that conventionally used for the main plasma species [3], we can write an equation for the impurity level  $N$  as a function of time as

$$N = S\tau_p^* + (N_0 - S\tau_p^*) \exp(-t/\tau_p^*), \quad (1)$$

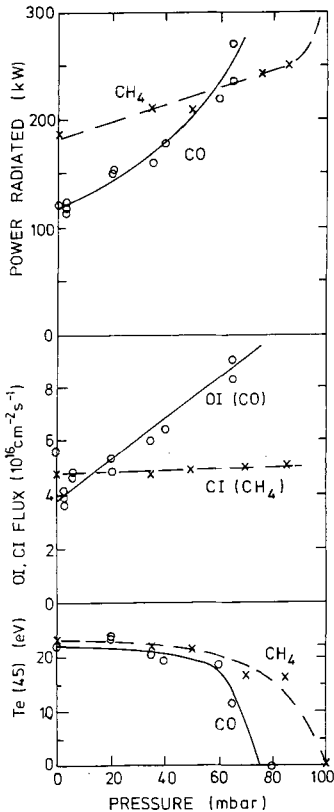


Fig. 4. Variation of the plasma edge temperature  $T_e$  (0.45 m), radiated power  $P_R$ , and oxygen recycling flux (OI) as a function of gas puffing rate. Gas puffing was through the test limiter at a radius of 0.46 m and parameters were measured at the end of the gas pulse, 1.3 s.

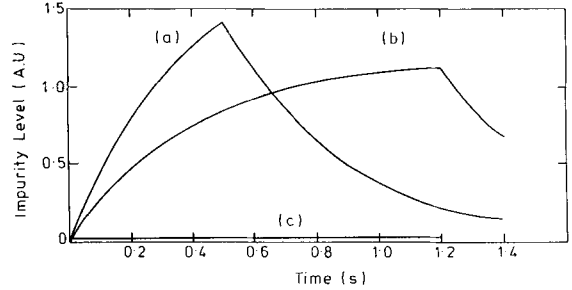


Fig. 5. Calculated time dependence of the impurity concentration using the global model (eq. (1)) with  $\tau_p = 5$  ms for different source function rates  $S$ , impurity pulse time  $t$  and recycling coefficients  $R$ . (a)  $S = 5$ ,  $t = 0.5$  s,  $R = 0.99$  (oxygen-like); (b)  $S = 3$ ,  $t = 1.2$  s,  $R = 0.99$  (oxygen-like); (c)  $S = 3$ ,  $t = 1.2$  s,  $R = 0.3$  (carbon-like).

where  $S$  is a constant impurity source function,  $N_0$  is the initial impurity level and  $\tau_p^*$  is given by

$$\tau_p^* = \frac{\tau_p}{1 - R}, \quad (2)$$

where  $\tau_p$  is the particle replacement time and  $R$  is the recycling coefficient.

In the case of oxygen,  $\tau_p^*$  is measured from the OI and the  $P_R$  decay after the CO influx is turned off, figs. 2a and 2b, and is typically 0.4 s. We can obtain  $\tau_p$  from calculations using the LIM code and the measured density and temperature profiles [11]. The calculated value depends directly on values of the cross-field diffusion and inward pinch used but typical values are 5 ms for both oxygen and carbon. Thus a value of  $R = 0.99$  is inferred for oxygen from eq. (2).

In the case of carbon, since we see no change in signal level during injection either of CO or CH<sub>4</sub> we cannot measure  $\tau_p^*$ . However, since we can calculate  $\tau_p$  from the LIM code and estimate  $R$  from the self-sputter yield, we can deduce  $\tau_p^*$ . Typical values are  $\tau_p^* = 7.7$  ms for carbon compared to the measured  $\tau_p^* = 400$  ms for oxygen. Examining eq. (1) we see that the low value of  $\tau_p^*$  leads to a low impurity level. Relative concentrations for oxygen and carbon calculated in this way are shown in fig. 5. They are in good agreement with the data on  $P_R$ , OI and CI shown in fig. 2. Because of the difference in  $\tau_p^*$  the increased level of carbon due to an external source is expected to be  $\sim \frac{1}{50}$  of the oxygen level, in agreement with experiment. The value of  $\tau_p$  will be larger for physically sputtered impurities than the thermal gas molecules because they will have energies of  $\sim 5$  eV and hence larger ionisation mean free paths. However, the effect of the low recycling coefficient of carbon relative to oxygen will be the same.

Laboratory experiments have shown that chemical sputtering of carbon by oxygen produces a CO molecule with a yield of  $\sim 1.0$  [2]. However during combined

hydrogen and oxygen ion bombardment it has been shown that oxygen can be released from the surface as water [12]. There is also recent evidence that oxygen can be physically sputtered from the surface [13]. There is thus some supporting evidence for the direct experimental result of fig. 2b that under these conditions the yield for production of CO must be  $\ll 1$ .

These observations are a remarkable illustration of the difference in behaviour of a high recycling and low recycling impurity. Similar examples of low recycling impurities recently reported are the injection of lithium pellets into TFTR [14] and the injection of methyl-boride into TEXTOR [15] which showed fuelling of the plasma by hydrogen without contamination by either boron or carbon. The fact that we can observe CIII local to the source but no significant change in CV seems to be strong indication that no carbon gets into the centre of the plasma, but only exists locally close to the source. The simple model discussed and the experimental results illustrate the difficulty of defining a "fuelling efficiency". The fraction of the injected impurities present in the plasma is a function of time and depends on  $R$  and  $\tau_p$  (and thus on  $D_{\perp}$  and the ionisation mean free path [16]).

## 5. Conclusions

The results indicate that the effective fuelling is low for both CH<sub>4</sub> and CO gas puffing. Moreover, the behaviour of carbon and oxygen are quite different. Earlier studies of the local transport show no significant difference between the two species. We have thus attributed the difference in the global behaviour to a markedly lower recycling coefficient for carbon than for oxygen. Such a difference is expected as one is a gas and the other a solid. An experimental estimate of  $R$  for oxygen is 0.99. Such an estimate is not possible for carbon because the increase in the carbon flux is below the detectable limit, but the results are consistent with  $R \approx 0.3$ . Such a low value means that the impurity concentration due to physical sputtering will also be less than is normally assumed. The results and discussion illustrate the difficulty of defining a "fuelling efficiency" for a given impurity species.

Finally, the rate of gas puffing has been varied from levels at which there is little effect on the plasma parameters and in which the impurity behaviour can be studied as a trace impurity, to the situation where the impurity dramatically alters first the local plasma conditions and finally the overall power balance of the discharge. The value of this type of experiment, as opposed to the case where the power density on a surface is varied, is that the impurity injection rate can be accurately controlled. Further studies of this type may cast new light on the processes occurring during the carbon bloom and on impurity-induced disruptions.

## References

- [1] G. Bertschinger, Spring Meeting of the Deutsche Physikalische Gesellschaft, Vorhandl DPG VI 21 (1986) p. 26.
- [2] J. Roth, in: Data Compendium for Plasma Surface Interactions, eds. R.A. Langley et al., Nuclear Fusion Supplement (1984) p. 72.
- [3] G.M. McCracken and P.E. Stott, Nucl. Fusion 19 (1979) 889.
- [4] M. Ulrickson et al., J. Nucl. Mater. 176 & 177 (1990) 44.
- [5] C.S. Pitcher et al., Nucl. Fusion 29 (1989) 1919.
- [6] G.M. McCracken et al., J. Nucl. Mater. 176 & 177 (1990) 191.
- [7] A. Pospieszczyk et al., J. Nucl. Mater. 162–164 (1989) 574.
- [8] B. Schweer et al., these Proceedings (PSI-10), J. Nucl. Mater. 196–198 (1992) 174.
- [9] J. Ongena et al., 16th Symp. on Fusion Technology, London, UK, 1990 (Elsevier, Amsterdam, 1991) vol. 1, p. 552.
- [10] W. Eckstein, Data on heavy ion reflection, Max Planck Institut Report IPP 9/61 (1987).
- [11] P.C. Stangeby, C. Farrell, S. Hoskins and L. Wood, Nucl. Fusion 28 (1988) 1945.
- [12] J. Roth, E. Vietzke and A.A. Haasz, Atomic and Plasma–Material Interaction Data for Fusion, ed. R.K. Janev, Nuclear Fusion Supplement (1991) p. 63.
- [13] P. Bogen and D. Rusbuldt, these Proceedings (PSI-10), J. Nucl. Mater. 196–198 (1992) 179.
- [14] J.A. Snipes, J.L. Terry and E.S. Marmar, Proc. 18th EPS Conf., Plasma Phys. Control. Fusion 3 (1991) 141.
- [15] H.G. Esser et al., these Proceedings (PSI-10), J. Nucl. Mater. 196–198 (1992) 231.
- [16] P.C. Stangeby, J. Nucl. Mater. 176 & 177 (1990) 51.